

International Journal of Pharmacology

ISSN 1811-7775





ISSN 1811-7775 DOI: 10.3923/ijp.2023.367.380



Research Article Remotely Rutin-Loaded into Liposomes for Efficient Encapsulation and Enhancement of Bioavailability and Brain Targeting *in vivo*

¹Chengxue Pan, ^{1,2}Yao Yang, ³Xiaoying Duan and ¹Haixia Li

Abstract

Background and Objective: Rutin exerts a potential application in brain diseases, but it is difficult to cross the blood-brain barrier (BBB) and its bioavailability is limited. A biocompatible liposome system of rutin using a remote loading strategy had developed by us. The present work aimed to evaluate its characteristics, bioavailability and brain targeting in vivo. Materials and Methods: Rutin liposome (rutin-lipo) was prepared by calcium acetate gradient combined with reverse evaporation method. Subsequently, the encapsulation efficiency (EE) of rutin was measured using centrifugal ultrafiltration, size distribution, zeta-potential and state of rutin were determined by laser particle size analyze and Fourier transform infrared spectrum (FT-IR), respectively. Moreover, drug release in vitro was evaluated by the dialysis method. After the methodology of HPLC was evaluated for detecting drug concentration in plasma and different tissues of mice, pharmacokinetic and biodistribution were measured. Furthermore, the relative uptake rate (Re) and peak concentration ratio (Ce) were calculated to assess the targeting performance of rutin-lipo. **Results:** The EE of rutin, average size and zeta-potential were $80.05\pm3.04\%$, 149.3 ± 7.7 nm and -4.1 ± 0.8 mV, respectively. The FT-IR revealed that rutin was effectively loaded into the liposomes and rutin-lipo possessed a higher cumulative drug release percentage than rutin. Moreover, rutin presents enterohepatic circulation and all pharmacokinetics parameters of rutin-lipo better than those of the solubilized rutin, including half-life of elimination $(t_{1/2/8})$, mean residence time (MRT), clearance rate (CL) and relative bioavailability (220.76%). Furthermore, the drug distribution of rutin-lipo was the most changed in the liver due to its Ce (2.9236) being the largest. Notably, the brain Re of rutin-lipo was 2.6429 although its Ce was 0.9629. **Conclusion:** Rutin-lipo significantly increased the bioavailability of rutin via enterohepatic circulation and had the brain targeting, thus, providing an attractive alternative for applications of rutin in brain diseases.

Key words: Rutin, remote loading liposome, bioavailability, enterohepatic circulation, brain targeting, tissue distribution

Citation: Pan, C., Y. Yang, X. Duan and H. Li, 2023. Remotely rutin-loaded into liposomes for efficient encapsulation and enhancement of bioavailability and brain targeting *in vivo*. Int. J. Pharmacol., 19: 367-380.

Corresponding Author: Haixia Li, School of Pharmaceutical Sciences, Zhengzhou University, Zhengzhou 450001, Henan, China Tel: +86 371 6778 1908 Fax: +86 371 6773 9546

Copyright: © 2023 Chengxue Pan et al. This is an open access article distributed under the terms of the creative commons attribution License, which permits unrestricted use, distribution and reproduction in any medium, provided the original author and source are credited.

Competing Interest: The authors have declared that no competing interest exists.

Data Availability: All relevant data are within the paper and its supporting information files.

¹School of Pharmaceutical Sciences, Zhengzhou University, Zhengzhou 450001, Henan, China

²Children's Hospital, Zhejiang University School of Medicine, Hangzhou 310006, Zhejiang, China

³First Affiliated Hospital of Henan University of Traditional Chinese Medicine, Zhengzhou 450099, Henan, China

INTRODUCTION

Rutin (3',4',5,7-tetrahydroxy-flavone-3-rutinoside), also named Vitamin P, quercetin-3-O-rutinoside, is a common dietary flavonoid with multiple pharmacological activities, such as antioxidant, anti-inflammation, protective effects on liver and blood vessels¹. The Dietary Supplement Label Database lists over 860 products containing rutin that are currently marketed in the US². However, the major disadvantage of rutin is its limited bioavailability, mainly caused by its tending to be insoluble in both water and oils (less than 0.13 and less than 0.25 mg g^{-1} , respectively)²-⁴. Therefore, significant research efforts have been devoted to nano-formulations for overcoming the determinant factor.

The biocompatible and biodegradable liposome is a promising candidate in the field of drug delivery because it can encapsulate both hydrophilic and hydrophobic drugs. Various methods are available for the preparation of liposomes^{5,6}, but disadvantages remain⁶⁻⁸, poorly water-soluble drugs are normally intercalated into the liposome bilayer if passive loading is employed, which cause a limited capacity and poor drug retention, i.e., resulting in burst drug release due to rapid extraction or exchange with plasma proteins after administration⁶⁻⁸. Thus, the active loading strategy of drug is often used to enhance the amount of entrapped drug and control drug release.

An acetate gradient is appropriate for the actively loading weak acidic drugs into liposomes by pH gradients⁹, such as pemetrexed¹⁰, cabazitaxel weak acid derivatives⁸. Rutin, a weak acidic drug, exerts a potential application in cerebral ischemia-reperfusion injury¹¹, neuroprotection¹², neurodegeneration and learning and memory impairment¹³. Clinically, rutin is used for cerebral haemorrhage, thrombophlebitis and adjuvant treatment of hypertension etc.². However rutin is difficult to cross BBB¹⁴. In the present study, based on our previous report of a liposome delivery system for rutin using remote loading strategy of calcium acetate gradient, the further investigation was carried out to explore its characteristics, bioavailability and brain targeting for utilizing the protective effect of rutin against brain diseases by circumventing conventional limitations.

MATERIALS AND METHODS

Study area: The study was conducted from January, 2021 to November, 2022 at School of Pharmaceutical Sciences, Zhengzhou University.

Study design

Preparation of remote loading rutin into liposomes: Blank liposomes were prepared by a reverse evaporation approach.

Briefly, phospholipid/cholesterol (5:1, w/w) was dissolved in the mixed solvent of ether/chloroform (2:1, v/v) to prepare an organic phase solution at a concentration of 40 mg mL⁻¹. Then, 5mL of calcium acetate aqueous solution (0.12 mol L^{-1}) was added dropwise into 15 mL of organic phase under an ultrasonic to form water in oil (W/O) emulsion solution. After the emulsion solution was removed organic phase under vacuum evaporation to form a colloidal state, it was hydrated by phosphate buffer solution (PBS) pH 7.4. Next, the mixture was continually vacuum evaporated for fully removing organic solvent and then further ultrasonicated using an ultrasonic probe (Ningbo Scientz Biotechnology Co., Ltd., Ningbo, Zhejiang, China) for 200 W, 30 times. Then, successive extrusion operation through a 450 and 220 nm pore size filter membrane for 3~4 times was performed to homogenize the resulting heterogeneous size of liposomes, after that blank liposomes were obtained.

For establishing calcium acetate gradient, the resulting blank liposomes were dialyzed 3 times with 3% sucrose water solution (10-fold volume) under magnetic stirring at room temperature, 1 hr per time. Then, the polyvinyl pyrrolidone (PVP) aqueous solution of rutin (rutin-PVP) was prepared according to the following method. Rutin/PVP (1:8, w/w) were dissolved in methanol, after methanol was removed, the solid was re dissolved in 1 mL of ultrapure water to give a final concentration of 5 mg mL⁻¹ of rutin. Finally, the remote loading of rutin into liposomes was achieved by co-incubation of 1 mL solution of rutin-PVP and 4 mL of blank liposomes at 50°C for 15 min.

Encapsulation efficiency (EE): After ultrafiltration centrifugation, the free rutin was measured by High-Performance Liquid Chromatography (HPLC) (Agilent Technologies, Palo Alto, California, USA) method according to the method described by Remanan and Zhu¹⁵ with some modifications. The conditions are as follows: Inertex C_{18} column (250×4.6 mm, particle diameter 5 μm), mobile phase methanol and 1% glacial acetic acid in water (32:68 v/v), detector wavelength 257 nm, flow rate 1.0 mL min⁻¹, injection volume 10 μL and column temperature 35°C. The total rutin was determined after adding 10% Triton X-100 solution to demulsify. The EE of rutin in liposomes was calculated by the following equation:

$$EE (\%) = \frac{W_{total} - W_{free}}{W_{total}} \times 100$$

where, W_{total} is the total amount of rutin and W_{free} is the free amount of rutin.

Characterization of formulation: The size distribution and zeta potential were analyzed using a Zetasizer Nano ZS-90 (Malvern, UK). The Fourier Transform Infrared (FT-IR) spectrum was used to characterize liposomes. The samples were milled and mixed with KBr, then compressed into a thin pellet for scan by FT-IR (Nicolet iS10 spectrometer, Thermo Scientific, Waltham, Massachusetts).

In vitro drug release: Dialysis method was applied to investigate the rutin release in vitro, the method of Asfour and Mohsen¹⁶ with little modification. As 2.0 mL of rutin-lipo suspension solution was transferred into a dialysis bag (MWCO 8~14 kDa) and immersed into 30 mL of phosphate buffer solution (PBS, pH 7.4) containing 0.5% SDS (w/v). The release system was continuously incubated under oscillation (100 r min⁻¹) at a temperature of 37°C. At each designated time point, 2 mL of release solution was withdrawn for measurement and 2 mL of medium was supplemented. The content of released rutin was measured by HPLC as described in encapsulation efficiency (EE). The cumulative release percentage of rutin was calculated and plotted. For control experiment, the same amount of drug in rutin raw material or rutin-PVP was used for dialysis after it was suspended or dissolved in aqueous solution under an ultrasonic bath, respectively.

Pharmacokinetic studies: Male Kunming mice (22±2 g) were obtained from Henan Laboratory Animal Center. All animal experiments were performed according to the national regulations and approved by the Institutional Animal Ethical Committee of Zhengzhou University. Mice were randomly divided into 2 groups: (1) Solubilized rutin and (2) Rutin-lipo. In the group of solubilized rutin, 10 mg of raw drug was dissolved in 2 mL of glycerol and 0.05 mL of Tween 80 under ultrasonic condition and then diluted to 10 mL with normal saline. After mice were kept fasting overnight, either solubilized rutin or rutin-lipo, containing 10 mg kg⁻¹ rutin, was injected via lateral tail vein. Blood samples were collected at designated time points (3 mice per point) to separate plasma and the plasma was stored at -20°C until further analysis. The plasma was deproteinized by vortex for 3 min with 5 time volume of acetonitrile:10% glacial acetic acid (20:1 v/v). It was then centrifuged at 12000 rpm for 15 min at 4°C and the supernatant liquid was separated and dried with nitrogen. The residue was then re-dissolved by mobile phase. After centrifugation, the supernatant was analyzed by HPLC to determine drug concentration.

Biodistribution and targeting of rutin: *In vivo*, biodistribution was studied together with pharmacokinetics

after mice were injected a single dose of solubilized rutin or rutin-lipo equivalent to 10 mg kg⁻¹ rutin (body weight). Briefly, at designated time points after administration, brain, heart, lung, liver, spleen and kidney were quickly dissected out and then washed in normal saline. Then, they were weighed and homogenized in normal saline in cold condition after blotted by filter paper. The homogenates were mixed with 5-fold volume of acetonitrile:10% glacial acetic acid (20:1 v/v). Next, the tissues samples were treated and the drug concentration were detected as stated in section of pharmacokinetic studies. The targeting of the formulation was evaluated by relative uptake ration (Re) and ratio of peak concentration (Ce). They were calculated according to the following equations¹⁷:

$$Re = \frac{AUC_{Rutin-lipo}}{AUC_{Solubilized\ rutin}}$$

$$Ce = \frac{\left(C_{max}\right)_{Rutin-lipo}}{\left(C_{max}\right)_{Solubilized rutin}}$$

where, AUC and C_{max} are the area under the concentration-time curve and the peak concentration of the drug, respectively.

Method validation: The HPLC method determining the drug concentration of plasma and tissues was evaluated by the specificity, selectivity, precision (intraday precision and interday precision), accuracy, stability and repeatability to ensure the validity, according to the method of Chinese pharmacopoeia for the analysis of biological samples. The solution of rutin at three different concentrations (low, medium and high) was individually and precisely added into the 100 µL solution of blank plasma or tissue homogenate to prepare biological samples, then they, five samples for each concentration, were vortexed and treated as stated in section of pharmacokinetic and tissue distribution studies. Next, they were examined for five replicates within one day and additionally on five consecutive days to evaluate the intraday and interday precision. The recovery was calculated according to the following equation, provided by Chinese pharmacopoeia for the analysis of biological samples:

Recovery (%) =
$$\frac{\text{Measured concentration}}{\text{Theoretical concentration}} \times 100$$

where, theoretical concentration corresponds to the true concentration of rutin at low, medium or high, measured concentration corresponds to rutin concentration calculated from the measured peak area according to standard curves of adding rutin to the matrix (plasma or solution of tissues

samples) and treated in relative recovery or standard curve of directly injecting rutin into a chromatographic column in absolute recovery. Finally, HPLC conditions of pharmacokinetic and tissue distribution were determined as mobile phase methanol and 1% glacial acetic acid in water (37:63 v/v), detector wavelength 360 nm, injection volume 20 μ L and other conditions same as described in EE.

Statistical analysis: The 3P97 software was applied to handle the data and fit pharmacokinetic parameters. And, all data were presented as Mean \pm Standard deviations of three replicate. Significant differences between means were determined by at a level of p<0.05.

RESULTS

EE, size, zeta-potential and stability of rutin-lipo: The schematic diagram of remotely loading rutin into liposome was shown in Fig. 1a. After rutin was loaded, the rutin-lipo (Fig. 1b) has a high EE ($80.05\pm3.04\%$) determined by HPLC result. And, its average size, polydispersity index (PDI) and zeta-potential were 149.4 ± 7.7 nm, about 0.2 and -4.1 ± 0.8 mV, respectively (Fig. 1c-d). The blank liposome exhibited smaller size (131.7 ± 6.6 nm), similar PDI and bigger zeta-potential (11.4 ± 1.5 mV) (Fig. 1e-f). The increasing size and the changing zeta potential of rutin-lipo suggested that rutin was loaded into liposomes. In addition, the rutin-lipo displayed good storage stability at 4° C, because there were no significant changes in particle size and EE for 4 weeks.

FT-IR spectrum: The typical stretching vibration peaks at 1131 cm⁻¹ for C-O, at 1630 cm⁻¹ for benzene ring skeleton and 3423 cm⁻¹ for associated OH were found in FT-IR spectrum of rutin, respectively (Fig. 2a). After being formulated by remote loading into liposomes composed of phospholipid, cholesterol and PVP, the characteristic peaks of C-O and associated OH were shifted to lower wavenumber 1119 and 3415 cm⁻¹, respectively and the characteristic peak of C-N was shifted to higher wavenumber 1437 cm⁻¹ (Fig. 2b), compared with rutin and rutin-PVP (Fig. 2c). In rutin-PVP, the typical stretching vibration peaks of PVP spectra were as follows: (1) 1421 cm⁻¹ corresponding to the C-N, (2) About 2925 cm⁻¹ corresponding to the saturated C-H₂ (Fig. 2c) and the association of -OH was attenuated compared with rutin (Fig. 2a), indicated by the higher wavenumber 3431 cm⁻¹ and weaker peak strength. These results suggested that the association state of rutin and nitrogen atom in PVP were changed in rutin-lipo, which may be caused by the alkaline environment generated by calcium acetate in liposome, i.e., driving force of remote loading.

In vitro **release:** Figure 3 showed that cumulative drug release percentage from raw rutin was $23.26\pm2.76\%$ in 12 hrs, it was $49.20\pm3.36\%$ in rutin-lipo. The significantly higher release percentage suggested that rutin-lipo can improve the release of poorly soluble rutin, thus it may be possible to enhance the bioavailiability of rutin. Comparing with the maximum cumulative release of rutin-PVP in the 10 hrs, i.e., $73.77\pm3.56\%$, the release of rutin from rutin-lipo was slower and sustained.

Quantification of rutin in plasma: At the same dose of 10 mg kg⁻¹ of rutin, the rutin in plasma was still detected at 8 hrs after i.v. injection of ruitin-lipo, but it decreased to be below detection limit after 3 hrs from very high plasma concentration in solubilized rutin (Fig. 4a). These results suggested that the drug concentration wasn't able to maintain stability in several hours for solubilized rutin, however, rutin-lipo possessed more stable plasma concentration and had sustained release properties.

The fitting results of plasma data showed that when the pharmacokinetic model was two-compartment, Akaike's Information Criterion (AIC) was minimum and comprehensive fit (r²) was maximum. The pharmacokinetic parameters using two-compartment model were collected in Table 1. The t_{1/2(8)} and MRT (MRT= AUMC/AUC) of rutin-lipo were longer than that of solubilized rutin, from 0.9897 to 3.030 hrs and from 1.428 to 4.372 hrs, respectively. The CL of rutin-lipo was less than that of solubilized rutin from 0.5581 mL/(kg h⁻¹) to $0.2528 \text{ mL/(kg h}^{-1})$. The areas under the concentration-time curve (AUC) of rutin-lipo and solubilized rutin were 39.56 and 17.92 hr/µg/mL, respectively. The relative bioavailability (Fr), the most important parameter to evaluate the efficacy of a preparation 18, was calculated according to the method described by Shi et al.19. The Fr of rutin-lipo was 220.76%.

Tissue distribution: Figure 4b-g showed the results of tissue distribution. The organ with the highest concentration was kidney in solubilized rutin group (7.6643 μg mL⁻¹), but it was liver in rutin-lipo group (18.2068 μg mL⁻¹) at 5 min post injection, suggesting that rutin might be rapidly transported to kidney and excreted in solubilized rutin, but be transported to liver in rutin-lipo. And except for liver and spleen, the drug concentration obviously decreased from substantially high concentration in 1 hr of administrating solubilized rutin, but it was relatively stable at each time point in rutin-lipo group. For liver, the drug concentration experienced the change of first decreasing and then increasing accumulation in both solubilized rutin and rutin-lipo, indicating the existence of hepatointestinal circulation. The drug concentration of the

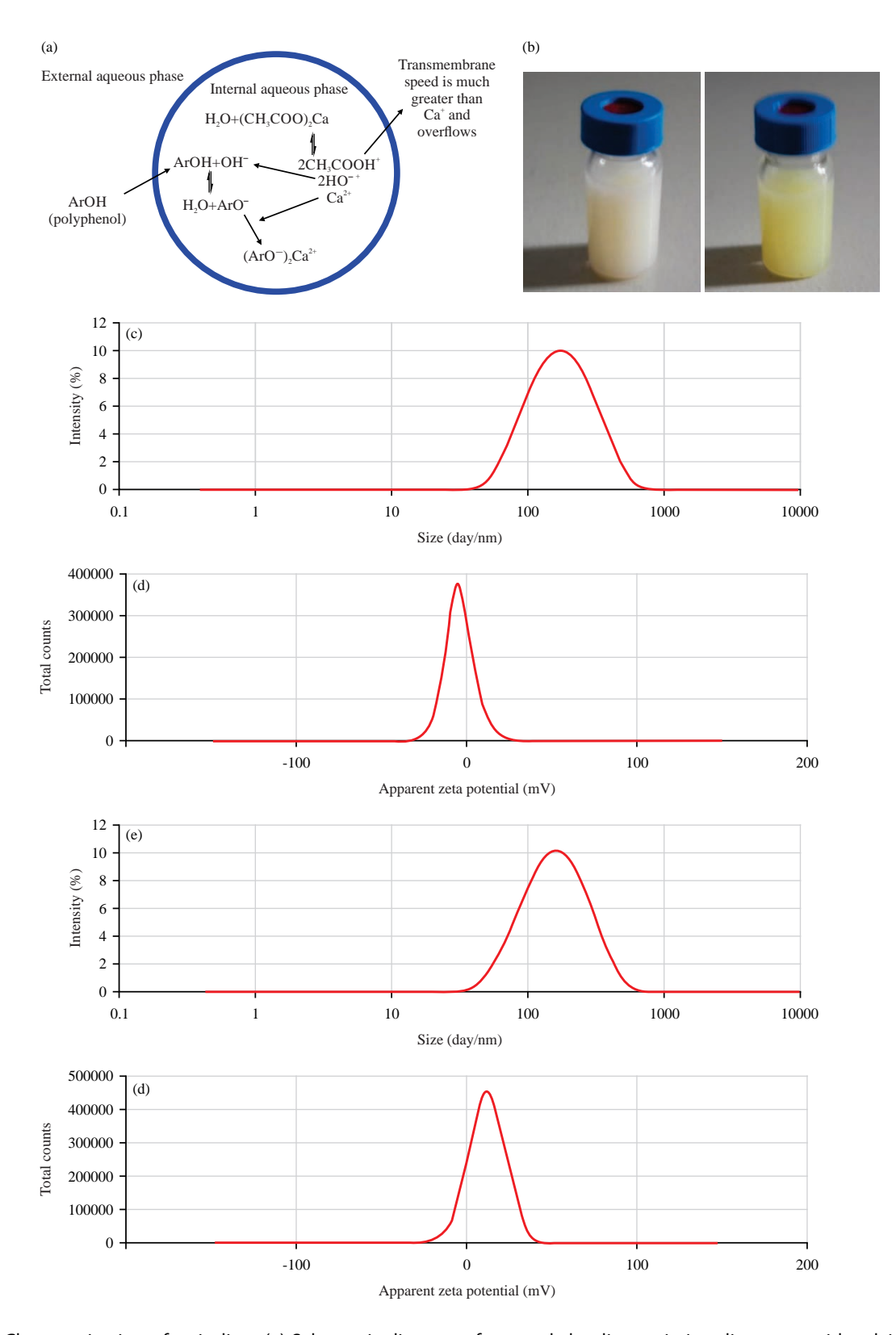


Fig. 1(a-e): Characterization of rutin-lipo, (a) Schematic diagram of remotely loading rutin into liposome with calcium acetate gradient method, (b) Images of liposomes, left to right: Blank liposome, ruitn-lipo, (c-d) Size distribution and zeta potential of ruitn-lipo and (e-f) Blank liposome

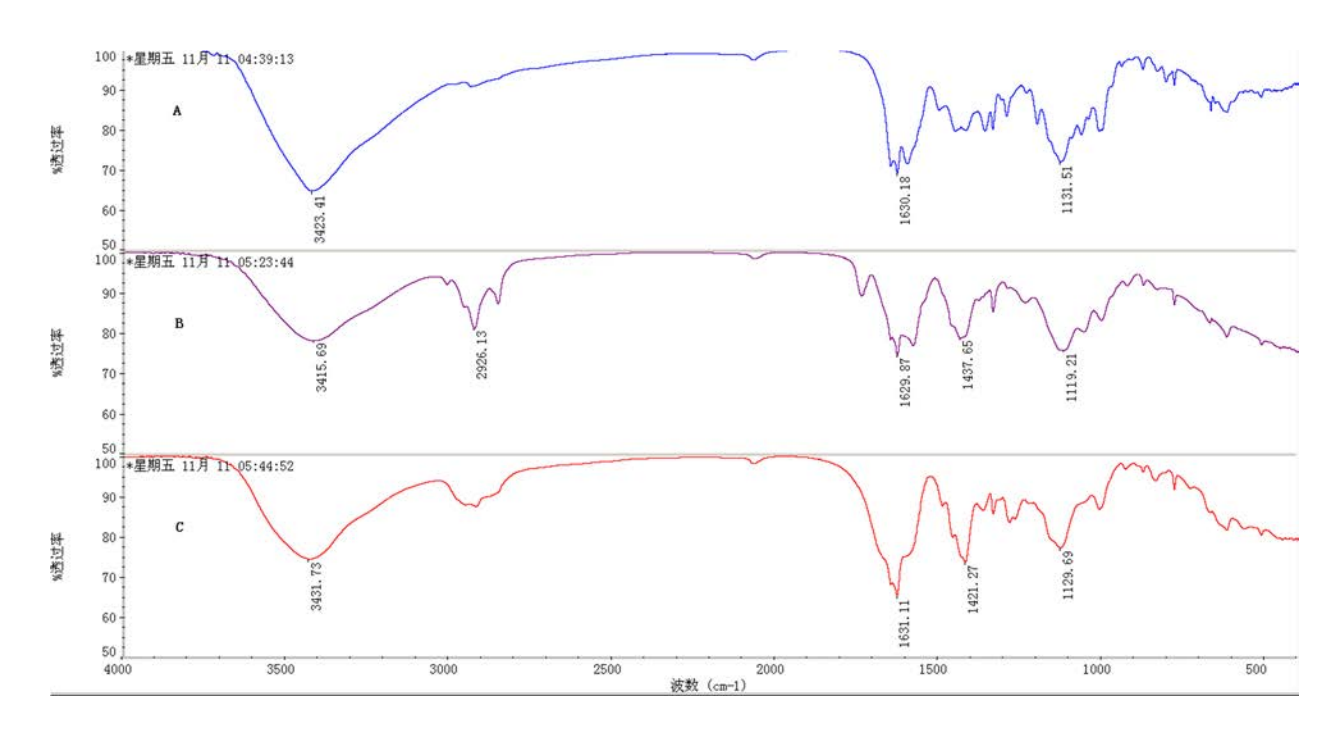


Fig. 2(a-c): Characterization of the FT-IR spectra, (a) Rutin, (b) Rutin-lipo and (c) Rutin-PVP

Prominent changes in rutin-lipo were that C-O and associated OH were shifted to lower wavenumber at 1119 and 3415 cm⁻¹, C-N was shifted to higher wavenumber at 1437 cm⁻¹, respectively, suggesting the association state of rutin and nitrogen atom were changed

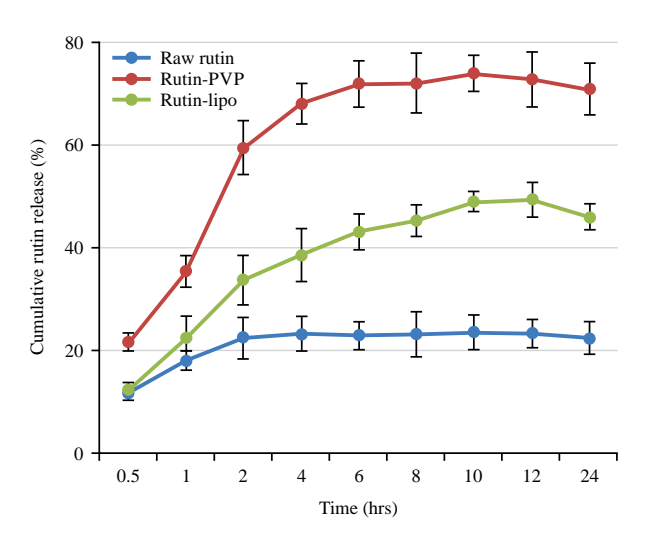


Fig. 3: *In vitro* release profiles of raw rutin, rutin-PVP and rutin-lipo by dialysis Each data represents the Mean±SD

spleen was ups and downs in both solubilized rutin and rutin-lipo, which may be related to hepatointestinal circulation. Notely, the drug concentration in brain remained a relatively high level in rutin-lipo rather than rapid disappearance in solubilized rutin due to the differences in absorption, distribution, metabolism and excretion of rutin.

Methodology: The specificity and selectivity were assessed by the resolution and peak purity of rutin, respectively. The results of HPLC chromatograms of blank plasma, blank plasma with rutin (adding rutin solution) and plasma of rutin-lipo group showed that the peak of rutin wasn't interfered with endogenous substances (Fig. S1) and was pure through diode

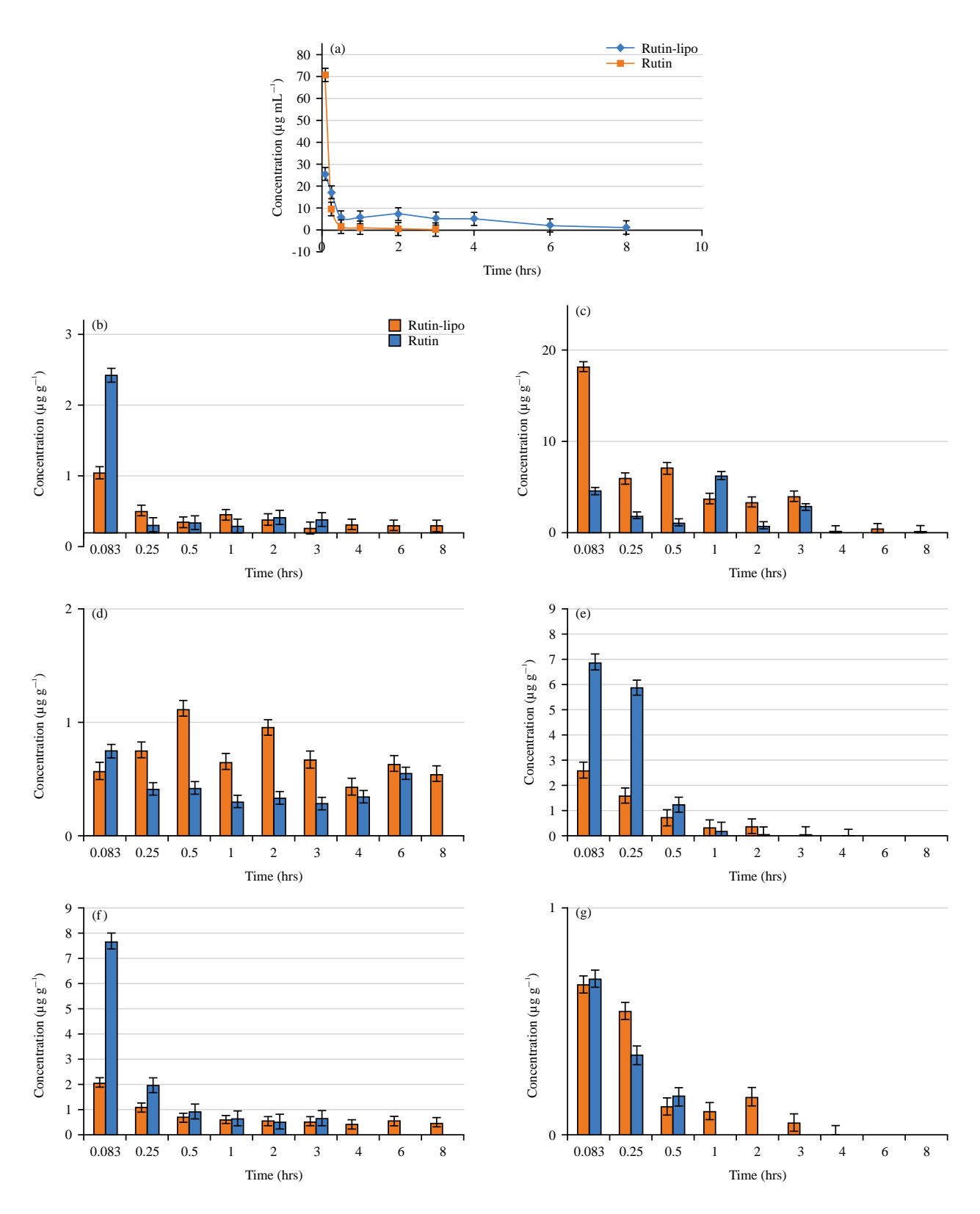


Fig. 4(a-g): Rutin concentration of plasma or tissues vs time, (a) Plasma, (b) Heart, (c) Liver, (d) Spleen, (e) Lung, (f) Kidney and (g) Brain

Mice were intravenously injected solution of solubilized rutin (rutin) or rutin-lipo at dose 10 mg kg $^{-1}$ body weight. Results are expressed as Mean \pm SD (n = 3)

Table 1: Plasma pharmacokinetics parameters of rutin after IV administration in mice at 10 mg kg^{-1}

Parameter	AUC (hr/μg/mL)	$t_{1/2(\beta)}(hr)$	CL (mL/(kg h ⁻¹))	AUMC (h²/μg/mL)	MRT (hr)	Fr (%)
Solubilized rutin	17.92	0.9897	0.5581	25.59	1.428	-
Rutin-lipo	39.56	3.030	0.2528	172.96	4.372	220.76

Table S1: Intraday precision and interday precision of rutin-lipo in plasma or different tissues

	Concentration (µg mL ⁻¹)	Intraday precision		Interday precision	
Tissue		Mean±SD	RSD(%)	Mean±SD	RSD (%)
Plasma	0.09045	0.09055±0.007	7.73	0.09085±0.0076	8.37
	4.523	4.518±0.14	3.09	4.575±0.34	7.43
	9.045	9.019±0.34	3.77	9.083 ± 0.46	5.06
Heart	0.09045	0.0913 ± 0.0061	6.68	0.09076±0.0071	7.82
	4.523	4.545±0.17	3.74	4.498±0.27	6.00
	9.045	9.018±0.43	4.77	9.031±0.23	2.55
Liver	0.09045	0.9031 ± 0.0403	4.46	0.09098±0.0068	7.47
	4.523	4.148±0.27	6.51	4.558±0.27	5.92
	9.045	9.039±0.53	5.86	9.038±0.42	4.65
Spleen	0.09045	0.09034±0.002	2.21	0.09024±0.0062	6.87
	4.523	4.566±0.28	6.13	4.496±0.08	1.78
	9.045	9.129±0.37	4.05	9.012±0.21	4.24
Lung	0.09045	0.09036 ± 0.002	2.21	0.09074±0.0076	8.38
	4.523	4.246±0.18	4.24	4.456±0.38	8.53
	9.045	9.293±0.56	6.03	9.193±0.46	5.00
Kidney	0.09045	0.09034±0.004	4.43	0.09014 ± 0.0063	6.99
	4.523	4.524±0.36	7.96	4.504±0.32	7.10
	9.045	9.103±0.52	5.71	9.069±0.42	4.63
Brain	0.09045	0.09034±0.003	3.32	0.09064 ± 0.0083	9.16
	4.523	4.556±0.4	8.78	4.646±0.24	5.17
	9.045	9.032±0.38	4.21	9.102±0.68	7.47

Table S2: Relative and absolute recovery of rutin in plasma or different tissues

Tissue	Concentration (µg mL ⁻¹)	Relative recovery (Mean±SD)%	Absolute recovery (Mean±SD) (%)
Plasma	0.09045	101.82±4.06	81.55±5.06
	4.523	88.88±3.04	85.18±2.04
	9.045	98.19±7.06	90.19±7.06
Heart	0.09045	91.03±5.01	79.03±3.01
	4.523	95.45±4.70	85.45±5.07
	9.045	101.80±2.23	90.18±1.23
Liver	0.09045	103.10 ± 3.63	91.31±6.93
	4.523	95.48±4.07	85.48±5.07
	9.045	100.09±5.20	82.09±3.52
Spleen	0.09045	91.34±4.72	81.34±2.62
	4.523	98.66±7.08	85.66±6.08
	9.045	93.19±1.21	90.59±5.22
Lung	0.09045	103.60±2.02	91.03±6.02
	4.523	92.46±6.08	75.15±4.08
	9.045	102.93±3.16	88.93±1.16
Kidney	0.09045	94.34±6.01	81.03±3.01
	4.523	94.44±3.26	79.14±5.86
	9.045	91.03±5.12	87.30±4.12
Brain	0.09045	90.14±3.03	81.03±2.73
	4.523	95.56±2.14	85.15±4.84
	9.045	100.20±3.58	90.22±6.48

array detector (DAD) purity analysis. So did the different tissues. The relative standard deviations (RSD) of intraday precision and interday precision were no more than 7.73 and 8.37% or 8.78 and 9.16% in plasma or different tissues,

respectively (Table S1) and the results of interday precision suggested that the rutin was stability in 5 days. The relative recovery was 88.88~103.60% in plasma and different tissues and the absolute recovery was greater than 75.15% in plasma

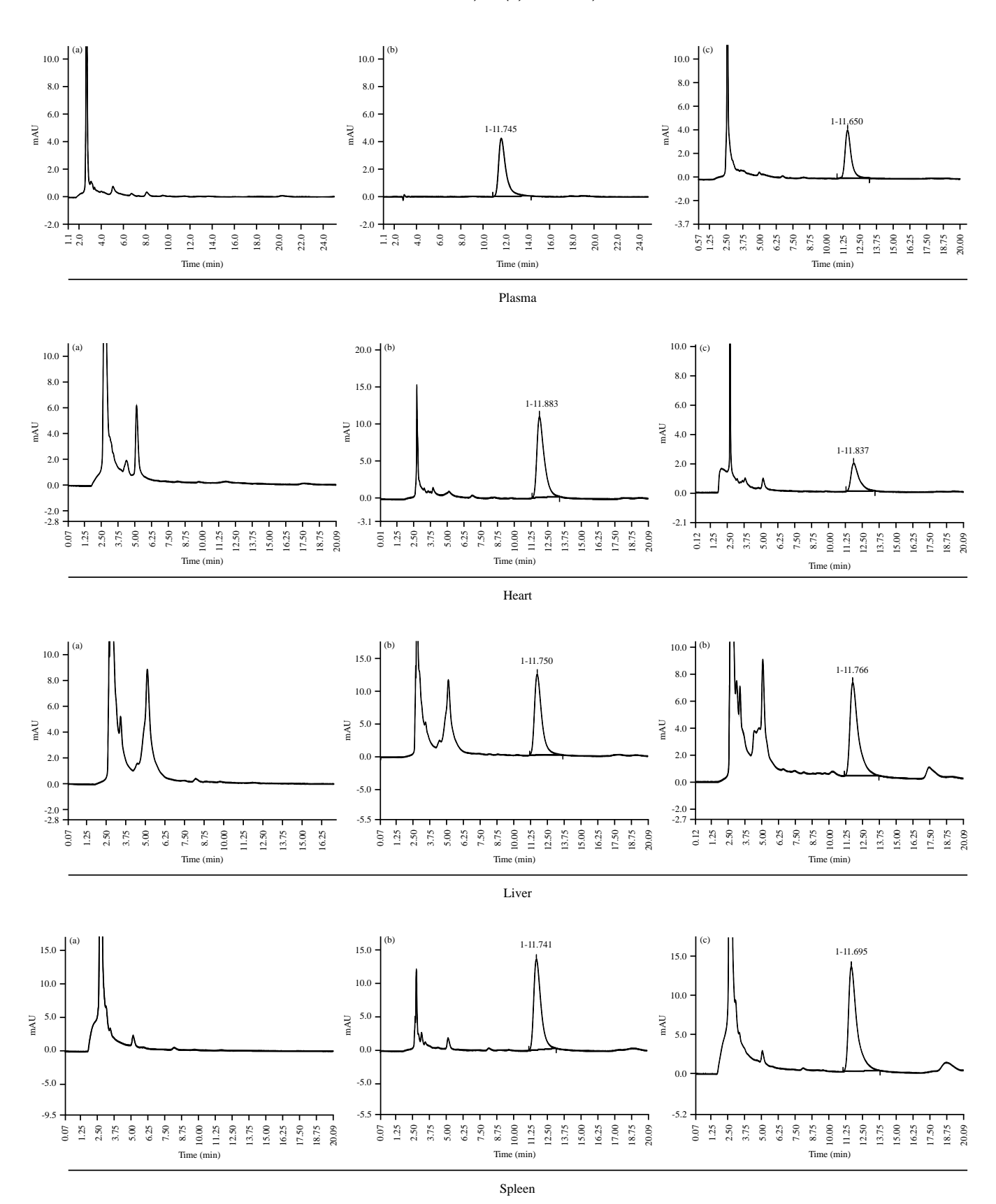


Fig. S1(a-c): Continue

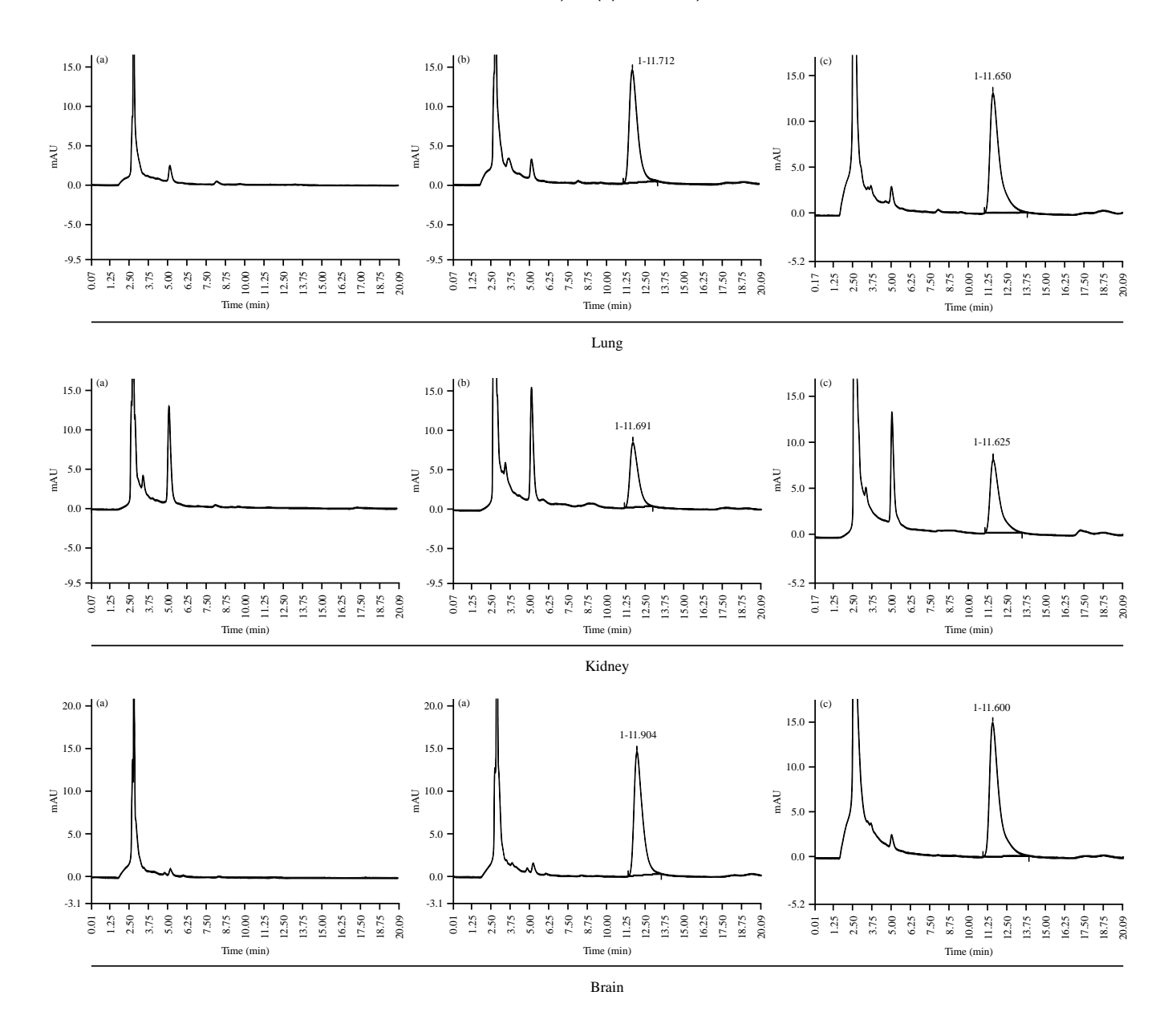


Fig. S1(a-c): HPLC chromatograms of plasma and different tissues, (a) Blank plasma or tissues samples, (b) Blank plasma or tissues samples with rutin and (c) Plasma or tissues samples of rutin-lipo

and different tissues (Table S2). The accuracy assessed by relative and absolute recovery showed that the described method was suitable for quantitative analysis. The standard curves of rutin in the plasma or different tissues were shown in Table S3. These results indicated that the HPLC analytical method possessed good specificity and selectivity, high precision, stability and accuracy.

Targeting performance: The Ce indicates the effect of the preparation changing the drug distribution, the larger the

Ce value, the more obvious the effect. The rutin-lipo enhanced the distribution of rutin in the liver and spleen due to their Ce value being 2.9236 and 1.5046, respectively (Table 2). The Re>1 of an organ or tissue indicates that it was targeted and the greater the Re value, the better the targeting effect. As shown in Table 2, the spleen is most targeted (Re = 5.1794) and followed by brain, liver, heart and kidney (Re = 2.6429, 2.0910, 1.6954 and 1.5879, respectively). Among them, the targeting of the brain and heart in rutin-lipo is fascinating due to their Ce<1.

Table 2: Targeting efficiency of rutin after IV administration in mice at 10 mg kg⁻¹

Tissue	C_{max} (µg g $^{-1}$)			AUC (hr/μg/g)		
	Solubilized rutin	Rutin-lipo	Ce	Solubilized rutin	Rutin-lipo	Re
Heart	2.2257	0.8380	0.3765	0.6330	1.0732	1.6954
Liver	6.2275	18.2068	2.9236	7.9469	16.6168	2.0910
Spleen	0.7472	1.1242	1.5046	1.0061	5.2110	5.1794
Lung	6.8751	2.6072	0.3792	2.5430	1.4879	0.5851
Kidney	7.6643	2.0521	0.2677	2.7037	4.2931	1.5879
Brain	0.3449	0.3321	0.9629	0.0980	0.2590	2.6429

Table S3: Standard curve of rutin in plasma and different tissues

Tissue	Equation	R ²	
Plasma*	A = 0.3915C+0.0695	0.9995	
Heart	A = 0.1870C + 0.0207	0.9993	
Liver	A = 0.1255C+0.0591	0.9994	
Spleen	A = 0.2509C-0.0471	0.9993	
Lung	A = 0.2421C+0.0765	0.9994	
Kidney	A = 0.1937C-0.0629	0.9994	
Brain	A = 0.2744C + 0.0386	0.9998	

^{*}Plasma concentration: mg×mL⁻¹

DISCUSSION

In the present study, it was found that rutin-lipo significantly increased the bioavailability of rutin and had the brain targeting. The rutin has been proven as a promising candidate in brain disease, such as improvement of spatial memory impairment¹³, anti-neurodegenerative diseases of Alzheimer's disease²⁰⁻²² and Parkinson's disease²³, inhibition of neuroinflammation and neurotoxicity²⁴. And rutin could exhibit a therapeutic role in cardio-cerebral vascular diseases, such as coronary heart²⁵, cerebral ischemia-reperfusion injury in ovariectomized rats¹¹ and ischemic stroke^{12,26}. However, its ability to cross the blood-brain barrier (BBB) is very weak. *In vitro* BBB model, the permeation of rutin across the BBB cell layer was only about 8%²⁷ and the permeability coefficient (P_{app}) of rutin was 3.4×10^{-6} cm sec⁻¹, suggesting that BBB permeation of rutin was neglected and it was difficult to cross BBB into the brain 14. To exert the treatment of brain disease, rutin must be present in the blood with high bioavailability and reach the cells in the brain. The results of the present study indicated that rutin-lipo can circumvent these limitations of rutin.

The strategy using various delivery systems for rutin has the potential to improve rutin bioavailability^{2,28}. Therefore, rutin has been prepared into various nano-formulations, such as rutin loaded chitosan-alginate nanoparticles²⁹, hybrid nanomaterials of MgO-NH₂-rutin³⁰, rutin-loaded ferritin nanoparticles³¹, amphiphilic triblock copolymer of PLGA-PEG-PLGA-loaded rutin nanorods³². Also, rutin-encapsulated chitosan nanoparticles were developed

for targeting the brain²⁶ and rutin was loaded into the DNA nanoflowers structure for achieving a robust inhibition of alzheimer disease²².

The amount of entrapped drug in the liposomes is an important factor for determining the therapeutic efficacy of the drug. Although remote drug loading method allows high drug encapsulation and prolonged release, the ionizable drugs of poorly aqueous solubility couldn't be actively loaded into the liposomal aqueous core in an aqueous solution due to low drug concentration^{7,8}. Consequently, a solvent-assisted active loading technology was developed to use miscible solvent assist the ionizable poorly soluble drugs to circumvent this predicament⁷. Similarly, PVP was employed in the current study to solubilize rutin in the loading water solution and promote the drug permeation into the liposomal core for active loading. After that, the EE of rutin-lipo was up to 80.05±3.04%.

Raw rutin showed limited release due to the relatively large crystalline particle size, this was consistent with the report of Wei *et al.*³³. However, its release was increased in rutin-PVP where rutin was present in an amorphous state (Fig. 3). Consistent to our results, previous studies also reported that rutin in an amorphous state exhibited faster release^{34,35}. The release of rutin from rutin-lipo was between raw rutin and rutin-PVP, which can be ascribed to rutin remote loading inside the liposomes. In agreement with our results, Bhattacherjee *et al.*³⁶ reported that the encapsulated rutin in nanoparticles was slower and sustained release than free rutin solution (acetonitrile solution of rutin).

The rutin-lipo showed slower elimination and more stable blood concentration (Fig. 4a), which may be explained by slow and sustained release of rutin from rutin-lipo (Fig. 3). More importantly, the Fr of rutin-lipo exhibited 220.76% increase compared with solubilized rutin. Therefore, rutin remote-loading in the liposomes prolong the circulation time of rutin in the body, thus improving its bioavailability.

The plasma concentration of rutin dropped to an extremely low level after 0.5 hr of injection of solubilized rutin (Fig. 4a). That may be caused by kidney excretion of large amount of rutin, suggested by its maximum uptake at 0.083 hr (5 min) after administration and then rapid decrease within 0.5 hr (Fig. 4f). However, in rutin-lipo group, kidney distribution of rutin was less (only 26.8% of solubilized rutin) and therefore drug excretion may be less (Fig. 4f), which resulted in slower decrease of drug concentration in plasma (Fig. 4a).

Choi et al.³⁷ proposed rutin was metabolized in the liver and most of it was then moved to the small intestines via the bile, after that rutin was transported to the large intestine, because after 1 hr intravenously injecting radiolabeled-rutin, the largest amount of the rutin was observed in the small intestine and followed by the liver, which was still a considerable amount of rutin and maximum accumulation was detected in the large intestine at 2 hrs after administration. Combination with our results of tissue distribution of solubilized rutin (Fig. 4c-f), we further speculated that after the kidney excreted a large amount of rutin, the liver metabolized the residual rutin in solubilized rutin. Thus, the effect of enterohepatic circulation may be a minor factor in solubilized rutin (Fig. 4a and c). However, it became major factor for rutin-lipo because the liver was the organ of the maximum concentration. Therefore, the plasma concentration of rutin rising again was more obvious in rutin-lipo. And the enterohepatic circulation of rutin-lipo is a benefit for the liver due to the protective effects of rutin on the liver1.

It is well known that liposomes can be swallowed up by macrophages after they are intravenously injected into the blood, so they can be concentrated in the liver and spleen tissues because they are rich in macrophages. This is consistent with our results, which showed the passive targeting in the liver and spleen of rutin-lipo due to their Ce>1 and Re>1 (Table 2). Notely, the active targeting of the brain and heart was driven by rutin-lipo in the present study due to their Ce<1 and Re>1 (Table 2). The main reasons for active targeting may be attributed to the increase of rutin-lipo's passively targeted to the liver (Re up to 5.18-fold) and the existence of enterohepatic circulation. After a large amount of the drug was absorbed by the liver, it was transported to the

small intestine and then entered again into the blood to enhance the bioavailability and cause the redistribution in the heart and brain.

The rutin-lipo can circumvent the rutin's disadvantages of the poor bioavailability and the weak ability to cross the BBB. Moreover, the liposome with high encapsulation efficiency is biocompatible and biodegradable. However, more investigation is necessary to validate the enhancement of therapeutic effect of rutin-lipo in one of models of brain disease.

CONCLUSION

Rutin-lipo significantly enhanced the bioavailability of rutin via enterohepatic circulation and realized the targeting of the heart and brain. Thus, rutin-lipo may provide a promising new strategy for increasing its cardi-cerebral protection activities, especially for the brain and is worthy of further study.

SIGNIFICANCE STATEMENT

This study uncovered the improvement of rutin liposome on the bioavailability and brain targeting via enterohepatic circulation. The rutin liposome has three advantages. Firstly, it can circumvent rutin's limitations of poor bioavailability and the weak ability to cross the blood-brain barrier. Secondly, the liposome is biocompatible and biodegradable and has high encapsulation efficiency due to employing the remote loading method. Thirdly, its enterohepatic circulation may be a benefit for rutin exerting its protective effect on the liver. Thus, the study may provide a promising new strategy for achieving the full potential of rutin as a functional ingredient of cerebral protection and it is worthy of further study in brain diseases.

ACKNOWLEDGMENT

This work was supported by the National Natural Science Foundation of China (Grant No. 81973727).

REFERENCES

- Semwal, R., S.K. Joshi, R.B. Semwal and D.K. Semwal, 2021. Health benefits and limitations of rutin-A natural flavonoid with high nutraceutical value. Phytochem. Lett., 46: 119-128.
- Gullón, B., T.A. Lú-Chau, M.T. Moreira, J.M. Lema and G. Eibes, 2017. Rutin: A review on extraction, identification and purification methods, biological activities and approaches to enhance its bioavailability. Trends Food Sci. Technol., 67: 220-235.

- 3. Wang, Q., J. Huang, C. Hu, N. Xia, T. Li and Q. Xia, 2017. Stabilization of a non-aqueous self-double-emulsifying delivery system of rutin by fat crystals and nonionic surfactants: Preparation and bioavailability study. Food Funct., 8: 2512-2522.
- 4. Bonechi, C., A. Donati, G. Tamasi, G. Leone and M. Consumi *et al.*, 2018. Protective effect of quercetin and rutin encapsulated liposomes on induced oxidative stress. Biophys. Chem., 233: 55-63.
- Al-Amin, M.D., F. Bellato, F. Mastrotto, M. Garofalo, A. Malfanti,
 Salmaso and P. Caliceti, 2020. Dexamethasone loaded liposomes by thin-film hydration and microfluidic procedures: Formulation challenges. Int. J. Mol. Sci., Vol. 21. 10.3390/ijms21051611.
- Ait-Oudhia, S., D.E. Mager and R.M. Straubinger, 2014. Application of pharmacokinetic and pharmacodynamic analysis to the development of liposomal formulations for oncology. Pharmaceutics, 6: 137-174.
- 7. Tang, W.L., W.H. Tang, A. Szeitz, J. Kulkarni, P. Cullis and S.D.Li, 2018. Systemic study of solvent-assisted active loading of gambogic acid into liposomes and its formulation optimization for improved delivery. Biomaterials, 166: 13-26.
- 8. Zhou, S., J. Li, J. Yu, L. Yang and X. Kuang *et al.*, 2021. A facile and universal method to achieve liposomal remote loading of non-ionizable drugs with outstanding safety profiles and therapeutic effect. Acta Pharm. Sin. B, 11: 258-270.
- Clerc, S. and Y. Barenholz, 1995. Loading of amphipathic weak acids into liposomes in response to transmembrane calcium acetate gradients. Biochim. Biophys. Acta (BBA)-Biomembr., 1240: 257-265.
- Bai, F., Y. Yin, T. Chen, J. Chen and M. Ge et al., 2018. Development of liposomal pemetrexed for enhanced therapy against multidrug resistance mediated by ABCC5 in breast cancer. Int. J. Nanomed., 13: 1327-1339.
- 11. Liu, H., L. Zhong, Y. Zhang, X. Liu and J. Li, 2018. Rutin attenuates cerebral ischemia-reperfusion injury in ovariectomized rats via estrogen-receptor-mediated BDNF-TrkB and NGF-TrkA signaling. Biochem. Cell Biol., 96: 672-681.
- 12. Chen, H., Y. He, S. Chen, S. Qi and J. Shen, 2020. Therapeutic targets of oxidative/nitrosative stress and neuroinflammation in ischemic stroke: Applications for natural product efficacy with omics and systemic biology. Pharmacol. Res., Vol. 158. 10.1016/j.phrs.2020.104877.
- 13. Zhang, L., Q. Zhao, C.H. Chen, Q.Z. Qin, Z. Zhou and Z.P. Yu, 2014. Synaptophysin and the dopaminergic system in hippocampus are involved in the protective effect of rutin against trimethyltin-induced learning and memory impairment. Nutr. Neurosci., 17: 222-229.
- Shimazu, R., M. Anada, A. Miyaguchi, Y. Nomi and H. Matsumoto, 2021. Evaluation of blood-brain barrier permeability of polyphenols, anthocyanins, and their metabolites. J. Agric. Food Chem., 69: 11676-11686.

- 15. Remanan, M.K. and F. Zhu, 2021. Encapsulation of rutin using quinoa and maize starch nanoparticles. Food Chem., Vol. 353. 10.1016/j.foodchem.2020.128534.
- 16. Asfour, M.H. and A.M. Mohsen, 2018. Formulation and evaluation of pH-sensitive rutin nanospheres against colon carcinoma using HCT-116 cell line. J. Adv. Res., 9: 17-26.
- 17. Ying, Z., Z. Rui-Zhi, C. You-Jun and L. Li-Juan, 2015. Effect of vinegar-baked *Bupleuri radix* on gentiopicroside in mice. Chin. J. Exp. Tradit. Med. Formulae, 21: 71-74.
- 18. Zhang, L., Q. Zhang, X. Wang, W. Zhang and C. Lin *et al.*, 2015. Drug-in-cyclodextrin-in-liposomes: A novel drug delivery system for flurbiprofen. Int. J. Pharm., 492: 40-45.
- Shi, F., Y. Zhao, C.K. Firempong and X. Xu, 2016. Preparation, characterization and pharmacokinetic studies of linalool-loaded nanostructured lipid carriers. Pharm. Biol., 54: 2320-2328.
- 20. Xu, P.X., S.W. Wang, X.L. Yu, Y.J. Su and T. Wang *et al.*, 2014. Rutin improves spatial memory in Alzheimer's disease transgenic mice by reducing Aβ oligomer level and attenuating oxidative stress and neuroinflammation. Behav. Brain Res., 264: 173-180.
- 21. Habtemariam, S., 2016. Rutin as a natural therapy for Alzheimer's disease: Insights into its mechanisms of action. Curr. Med. Chem., 23: 860-873.
- 22. Ouyang, Q., K. Liu, Q. Zhu, H. Deng and Y. Le *et al.*, 2022. Brain-penetration and neuron targeting DNA nanoflowers co-delivering miR-124 and Rutin for synergistic therapy of Alzheimer's disease. Small, Vol. 18. 10.1002/smll.202107534.
- 23. Enogieru, A.B., W. Haylett, D.C. Hiss, S. Bardien and O.E. Ekpo, 2018. Rutin as a potent antioxidant: Implications for neurodegenerative disorders. Oxid. Med. Cell. Longevity, Vol. 2018. 10.1155/2018/6241017.
- Magalingam, K.B., A. Radhakrishnan and N. Haleagrahara, 2016. Protective effects of quercetin glycosides, rutin, and isoquercetrin against 6-hydroxydopamine (6-OHDA)-induced neurotoxicity in rat pheochromocytoma (PC-12) cells. Int. J. Immunopathol. Pharmacol., 29: 30-39.
- 25. Lv, L., Y. Yao, G. Zhao and G. Zhu, 2018. Rutin inhibits coronary heart disease through ERK1/2 and Akt signaling in a porcine model. Exp. Ther. Med., 15: 506-512.
- Ahmad, N., R. Ahmad, A.A. Naqvi, M.A. Alam and M. Ashafaq et al., 2016. Rutin-encapsulated chitosan nanoparticles targeted to the brain in the treatment of cerebral ischemia. Int. J. Biol. Macromol., 91: 640-655.
- 27. Yang, Y., L. Bai, X. Li, J. Xiong, P. Xu, C. Guo and M. Xue, 2014. Transport of active flavonoids, based on cytotoxicity and lipophilicity: An evaluation using the blood-brain barrier cell and Caco-2 cell models. Toxicol. *In vitro*, 28: 388-396.
- Ghanbari-Movahed, M., A. Mondal, M.H. Farzaei and A. Bishayee, 2022. Quercetin- and rutin-based nanoformulations for cancer treatment: A systematic review of improved efficacy and molecular mechanisms. Phytomedicine, Vol. 97. 10.1016/j.phymed.2021.153909.

- 29. Surendran, V. and N.N. Palei, 2022. Formulation and characterization of rutin loaded chitosan-alginate nanoparticles: Antidiabetic and cytotoxicity studies. Curr. Drug Delivery, 19: 379-394.
- Singh, T.A., M. Kundu, S. Chatterjee, S.K. Pandey and N. Thakur *et al.*, 2022. Synthesis of Rutin loaded nanomagnesia as a smart nanoformulation with significant antibacterial and antioxidant properties. Inorg. Chem. Commun., Vol. 140. 10.1016/j.inoche.2022.109492.
- 31. Yang, R., Y. Liu, C. Blanchard and Z. Zhou, 2018. Channel directed rutin nano-encapsulation in phytoferritin induced by guanidine hydrochloride. Food Chem., 240: 935-939.
- 32. Saha, S. and A. Mishra, 2022. Rutin-loaded polymeric nanorods alleviate nephrolithiasis by inhibiting inflammation and oxidative stress *in vivo* and *in vitro*. Food Funct., 13: 3632-3648.
- 33. Wei, Q., C.M. Keck and R.H. Müller, 2017. Preparation and tableting of long-term stable amorphous rutin using porous silica. Eur. J. Pharm. Biopharm., 113: 97-107.

- 34. Koval'skii, I.V., I.I. Krasnyuk, I.I. Krasnyuk Jr, O.I. Nikulina and A.V. Belyatskaya *et al.*, 2014. Studies of the solubility of rutin from solid dispersions. Pharm. Chem. J., 47: 612-615.
- 35. Lee, I.L.W., J. Li, X. Chen and H.J. Park, 2017. Fabrication of electrospun antioxidant nanofibers by rutin-pluronic solid dispersions for enhanced solubility. J. Appl. Polym. Sci., Vol. 134. 10.1002/app.44859.
- 36. Bhattacherjee, A., K. Dhara and A.S. Chakraborti, 2016. Argpyrimidine-tagged rutin-encapsulated biocompatible (ethylene glycol dimers) nanoparticles: Synthesis, characterization and evaluation for targeted drug delivery. Int. J. Pharm., 509: 507-517.
- 37. Choi, M.H., J.K. Rho, J.A. Kang, H.E. Shim and Y.R. Nam *et al.*, 2016. Efficient radiolabeling of rutin with ¹²⁵I and biodistribution study of radiolabeled rutin. J. Radioanal. Nucl. Chem., 308: 477-483.